

EVALUATION OF THE INFLUENCE OF ELECTROMAGNETIC RADIATION ON THE STRUCTURAL HEALTH MONITORING METHOD BASED ON THE ELECTROMECHANICAL IMPEDANCE MEASUREMENTS

Tsuruta, Karina Mayumi, kmtsuruta@mecanica.ufu.br
Moura Junior, José dos Reis Vieira, mourajr@mourajr.com
Palomino, Lizeth Vargas, lypalomino@mecanica.ufu.br
Steffen Junior, Valder, vsteffen@mecanica.ufu.br
Rade, Raquel Satini Leandro, rslr@ufu.br
Rade, Domingos Alves, domingos@ufu.br

Faculdade de Engenharia Mecânica – Universidade Federal de Uberlândia - UFU
Avenida João Naves de Avila, 2121, Campus Santa Mônica, CEP 38400-902, Uberlândia - MG

Abstract. Structural health monitoring (SHM) is the process of damage identification in mechanical structures which encompasses four main phases: damage detection, damage localization, evaluation of damage extent and prognosis of residual life. Among the various existing SHM techniques, the one based on electromechanical impedance measurements has been regarded as one of the most effective, especially in the identification of incipient damage. This technique consists in measuring, with the help of a piezoelectric transducer bonded to the monitored structure, the so-called electromechanical impedance function which depends on the physical features of the structure (stiffness, damping and inertia). Should damage occur, those characteristics change and, as a result, information about damage can be perceived in the impedance measurements. For the success of monitoring, the measurement system must be robust enough with respect to environmental influences from different sources, in such a way that correct and reliable decisions can be made based on measurements. The environmental influences become more critical in some circumstances, especially in aerospace applications, in which extreme conditions are frequently encountered. In this paper the influence of electromagnetic radiation affecting the piezoelectric transducers and leading cables on impedance measurements is examined in laboratory. An aluminum beam, subjected to an electromagnetic field generated by a coil, is used as the monitored structure. Damage is simulated by adding mass to the structure. Two PZT patches are bonded to the structure. The mass and the applied electromagnetic field are varied. For each test condition, the differences between the impedance measurements in two states: without damage and with damage are compared. Conclusions are drawn regarding the influence of the electromagnetic field intensity on the monitoring effectiveness of the electromechanical impedance technique.

Keywords: Electromechanical Impedance; Structural health monitoring; Damage detection.

1. INTRODUCTION

SHM techniques have been receiving ever growing interest in aerospace and civil structures, vehicles and machines lately (Rutherford *et al.*, 2007). Among the SHM techniques, the method based on the electromechanical impedance is considered to be one of the most promising (Park *et al.*, 2003). It is a nondestructive method which explores the electro-mechanical coupling property of piezoelectric materials to monitor the occurrence and evolution of structural damage. The application of this technique consists in bonding piezoelectric materials, more frequently in a form of thin patches, to the monitored structure. The electromechanical behavior of this system can be characterized by the electromechanical-impedance, which is a function of frequency, defining the ratio between the input voltage and the electrical current. This function depends also upon the mechanical features (inertia and stiffness of the base structure). Thus, through the variations observed in the electromechanical impedance, it is possible to assess information about structural changes induced by damage. This possibility is due to the electrical impedance of the PZT patch being directly associated with the mechanical impedance of structure to which it is bonded. By using the same piezoelectric element as sensor and actuator, a smaller number of components and cables has been developed (Park *et al.*, 2003).

For the monitoring success of this technique, the system must be robust to environmental variations from different sources (Moura Jr, 2004; Moura Jr. and Steffen Jr., 2006). Otherwise, environmental changes could influence the measurements, undermining the reliability of the procedure and preventing the use of metrics associated with the method. Moreover, the process of monitoring the structural integrity can identify a situation of false positive during the evaluation of aircraft structures. So, it is necessary to evaluate the effects caused by electromagnetic fields and the possibility of occurrence of this type of diagnosis. For this purpose an aluminum beam was used subject to a magnetic field, and to simulate the damages, masses are added to the structure.

2. ELECTROMECHANICAL IMPEDANCE METHOD

The basic concept of this approach is to observe the variations in structural mechanical impedance of the monitored structure caused by the presence of damage. For this purpose, the method explores the electromechanical coupling of piezoelectric materials (most frequently small PZT patches) bonded to the host structure. By measuring the electromechanical impedance, which is represented by a frequency complex-valued function, and comparing to a baseline measurement, one can qualitatively determine that damage has occurred (Park *et al.*, 2003; Liang *et al.*, 1994). In a further, more involved step, a scalar metric can be defined to quantify the differences between the impedance functions in two different states and can be used to evaluate the damage severity and its evolution.

One of the main features of the electromechanical impedance technique is that it operates in high-frequency ranges (above 30 kHz) with typically short wavelengths. This fact makes the technique effective in monitoring incipient damage.

To obtain the electromechanical impedance the PZT patch is excited with very low alternating voltages (lower than 1 V), generating high-frequency mechanical waves, in such a way that the dynamic response of the structure reflects only a very small localized area around the transducer. This response returns back to the sensor in the form of electrical signal. The electromechanical impedance is thus obtained as a transfer function relating the excitation voltage and the response electrical current.

Fig. 1 shows a classical one-dimensional electro-mechanical model of the impedance-based structural health monitoring system, in which the parameters M, K and C designate the inertia, stiffness and damping of the host structure.

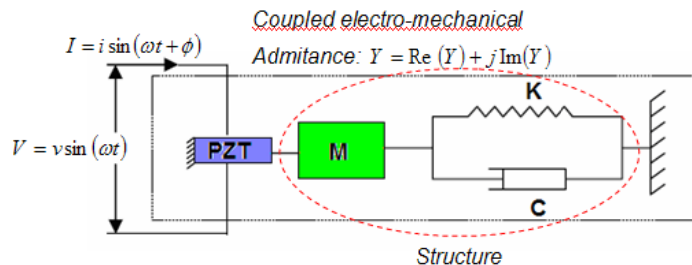


Figure 1. One-dimensional model used to represent a structural system excited by a PZT.

Using a wave propagation approach, Liang *et al.* (1994) demonstrated that the admittance (inverse of the impedance) $Y(\omega)$ of the electromechanical system is given by:

$$Y(\omega) = \frac{a^2}{Z_p + Z_s} \quad (1)$$

where, v is the input voltage amplitude; i is the output current amplitude; a is the geometric constant of the PZT; and Z_p and Z_s are the PZT's and structure's mechanical impedances, respectively, E is the complex Young's modulus of the PZT in x direction under zero electric field, d is the piezoelectric coupling constant in x direction, ϵ_0 is the dielectric constant at zero stress and $\tan \delta$ is the dielectric loss tangent of the PZT.

Electromechanical impedance functions can be experimentally obtained by signal processing of input voltage and output current signals using the specially adapted equipment known as impedance analyzer, which is illustrated in Fig. 2.



Figure 2. Impedance analyzer HP 4194A

The plots of the responses of impedance provide qualitative information about the presence of damage. While

the quantitative information can be provided by scalar values named damage metrics, which are computed from the impedance signals corresponding to two different states. This scalar value used in this paper is described as the "root mean square deviation" as defined by Sun *et al.* (1995) as:

$$M = \sum_{i=1}^n \sqrt{\frac{[\text{Re}(Z_1(\omega_i)) - \text{Re}(Z_2(\omega_i))]^2}{[\text{Re}(Z_1(\omega_i))]^2}} \quad (2)$$

where M is the damage metric and $\text{Re}(Z_1)$ and $\text{Re}(Z_2)$ are the real parts of the impedance at two different conditions, one of them considered as the baseline. The choice of the real part of the impedance functions for computing the damage metric is discussed and justified by Raju (1997).

3. METHODOLOGY

The methodology adopted in the study reported here consists in testing an aluminum beam under electromagnetic field. The damage was simulated adding mass (1g and 2 g) on the beam at the point hatched, shown in the fig. 3.

The specimen bar used has 0.3 m length, approximately. Two piezoelectric transducers, with $0.01 \text{ m} \times 0.02 \text{ m}$ and 0.127 mm thickness were bonded to the specimen surface. One PZT was bonded near to one of its extremity (PZT1) and another at the center (PZT 2) of the beam, as illustrated in the Fig. 3.

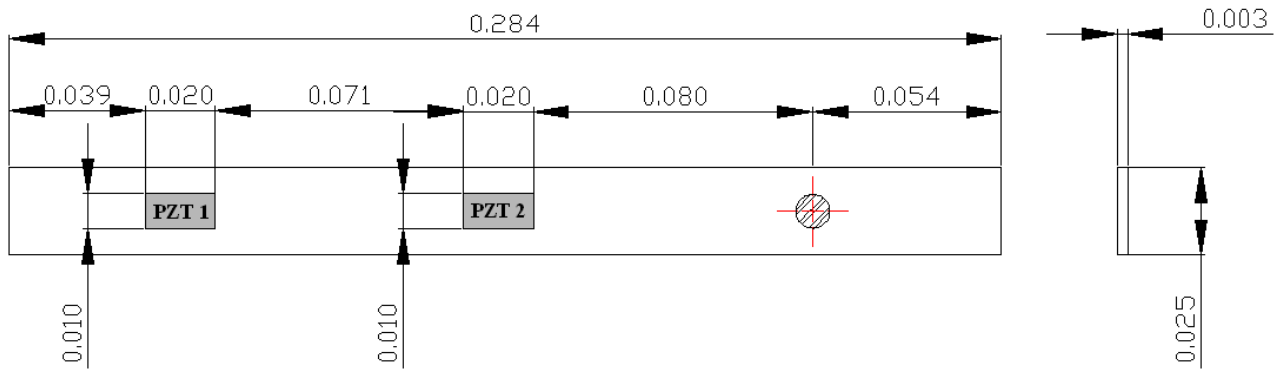
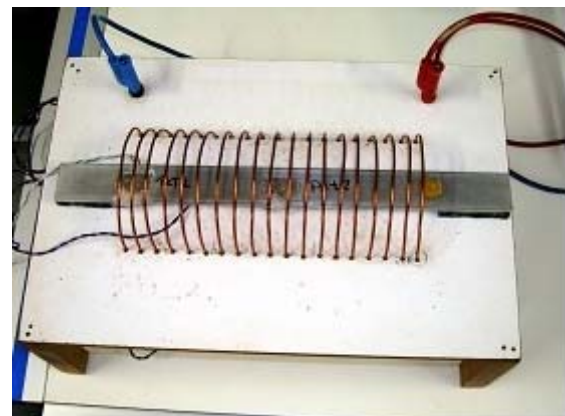


Figure 3. Geometry of the specimen and position of the PZT's.

The frequency band used to analyze the beam was A: 24 kHz - 34 kHz and B: 34 kHz - 40 kHz. The impedance signal acquisition at the tests under magnetic field influence used the following parameter at the impedance analyzer (Figure 2): output voltage: 1V and the mean number: 8. The figures 4(a) and 4(b) show the experimental apparatus used at the experiments.



(a)



(b)

Figure 4. Experimental apparatus: (a) Experimental assembly; (b) Aluminum beam inside the coil field generator and added mass.

For generation of the electromagnetic field was applied in the cooper coil by two different voltages: 2 V and 4 V. According to the Eq. 3, obtained from the Biot-Savard and Ampère laws, the values of the field generated can be easily computed.

$$B = \frac{\mu_0 N I_c}{2R} \quad (3)$$

where $\mu_0 = 1.2566 \times 10^{-6}$ Tm/A (magnetic constant), $N = 18$ turns, $I_c = Voltage/0,5 \Omega$, $R = 0.04$ m (average radius of the turns). The voltage values used were 2 e 4 Volts. Thus, from Eq. 3, the electromagnetic fields B were: 1.13094×10^{-3} T and 2.26188×10^{-3} T, respectively.

In the Table 1 the parameters adopted for the tests are showed, as explained before, two PZT patches, two masses, two voltages and two frequency ranges were used at the experiments.

Table 1. Feature of the experiments.

PZT Patch	Mass Added	Voltage	Frequency Range
PZT 1 / PZT 2	-	0	A / B ⁽¹⁾
PZT 1 / PZT 2	1 g	2 V	A / B ⁽¹⁾
PZT 1 / PZT 2	2 g	4 V	A / B ⁽¹⁾

⁽¹⁾: A: 24 kHz - 34 kHz and B: 34 kHz - 40 kHz.

For each experiment, an analysis of the impedance signals was made: baseline *versus* baseline, baseline *versus* impedance function measured after adding mass and changing the magnetic field applied. Here, the term baseline designates the healthy condition (before adding mass or applying the electric field). The first comparison was made to evaluate the influence of uncontrolled environmental factors or measurement noise on the impedance signals. The second one was made to detect damage caused by the added mass, thus each value of the damage metric was calculated using the Eq. 2.

4. DISCUSSION AND RESULTS

According to the methodology, the specimen was tested under a magnetic field, and measurements of electromechanical impedance were made before and after applying the magnetic field and added mass to the beam. To obtain the damage metric, just the real part of the impedance functions was treated according to Eq. 2. The impedance signals obtained in the several conditions were compared: baseline \times baseline and baseline \times after adding mass and after applying a magnetic field.

After analysis of the impedance function of the PZT patch 2 and frequency band B, showed incoherent results and peaks, because the data obtained in the experiments are corrupted, so it was decided to use just the frequency band A.

The results obtained for the PZT patch 2 are showed in the Fig. 5, 6 and 7. In the Fig. 5(a), 5(b), 6(a) and 6(b), where the real part of the impedance functions are showed. The first plot is a comparison between the data obtained without the addition of mass in the beam, but the electromagnetic field is varied, and the others graphics show a comparison of impedance function with addition of mass, but the voltage is 0 V, 2 V and 4 V, respectively. Analyzing the results, the first graphic show that there is no difference between the signals obtained in different conditions of magnetic field, showing that this environment did not affect the impedance function.

In Fig. 5 (b), 6 (a) and 6 (b), it is perceived that the impedance function measure after removing the mass and adding mass with 1 g and 2 g each time has a significant modification, and to quantify the change it was used the damage metric (Eq. 2). Herewith the Fig. 7(a) was obtained in this plot are the three clear groups which could be easily separable, due to the mass addition: 0, 1 g and 2 g. And with this groups it is possible to construct a box plot graphic with the values of damage metric showed in the Fig. 7(b), it is easy to distinct the different stages of mass added on the structure, which indicates that the electromechanical impedance measurements could detect damage under magnetic field. And the standard deviation of the mean value of the damage metric at the different stages showed in the figure 7 (b) might be caused by the noise from the environment.

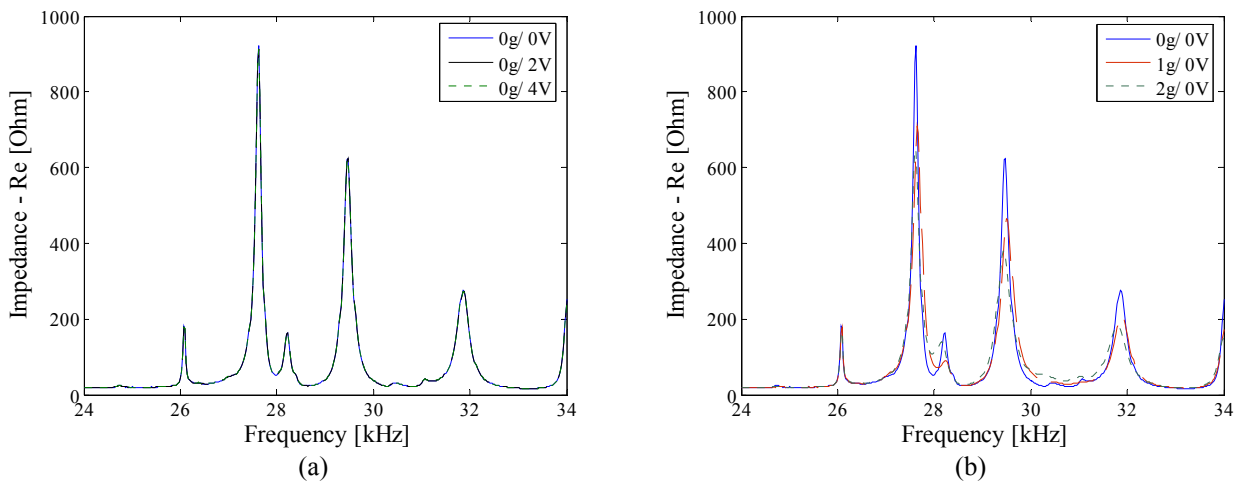


Figure 5. (a) Real part of the impedance function, varying the electromagnetic field (0 V, 2 V and 4 V); (b) Real part of the impedance function, varying the mass added on the structure and the electromagnetic field was constant (0 V).

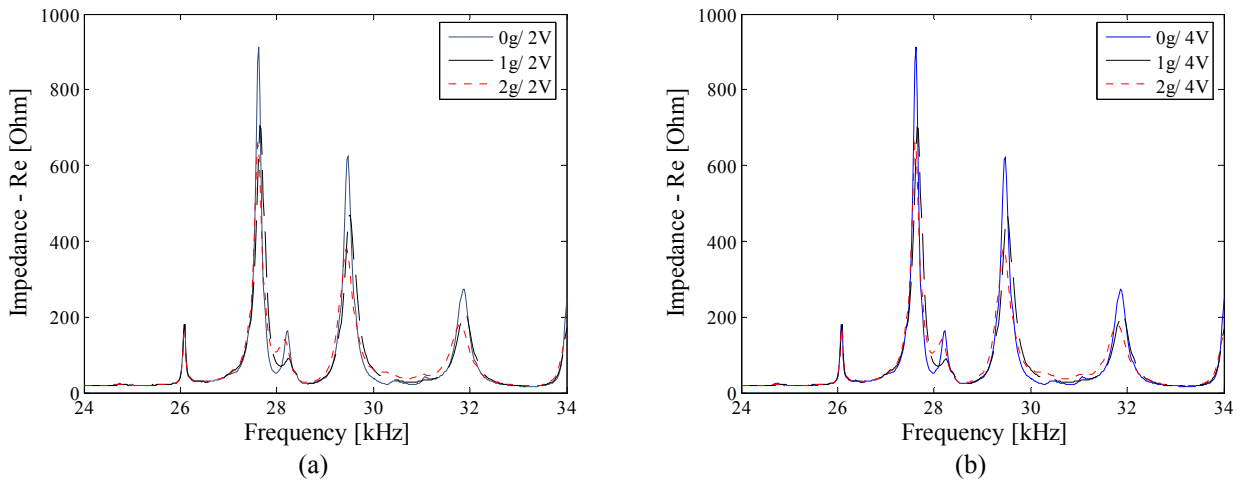


Figure 6. (a) Real part of the impedance function, varying the mass added on the structure and the electromagnetic field was constant (2 V); (b) Real part of the impedance function, varying the mass added on the structure and the electromagnetic field was constant (4 V).

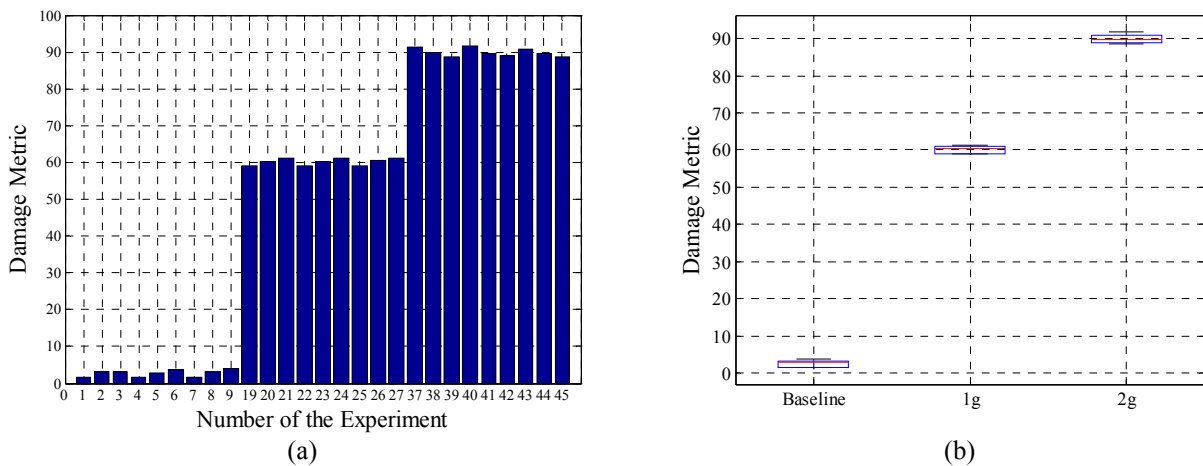


Figure 7. (a) Damage metrics for the experiments in the electromagnetic field environment; (b) Box plots of the damage metrics.

The Table 2 presents the values of the damage metrics after added mass on the structure with different magnetic field as explained in the methodology in the Table 1, where DM is the results of the equation of damage metric (Eq.2). And these results are used to building a meta-model for verification of the electromagnetic field effect. The results presented in Fig. 8(a) and 8(b) are for the analysis of the main effect, it shows that the greatest contribution of the isolated effect of the mass than the electric field. Observing the graphic of cross effects (Fig. 8(b)), it is possible to notice that the voltage presents a slight inclination and the mass presents a great variation.

Tabela 2. Damage metric values for PZT Patch 2 and frequency band A.

Exp. Number	Mass [g]	Voltage [V]	DM
1	0	0	1.55
2	0	2	2.98
3	0	4	3.06
4	1	0	59.09
5	1	2	60.14
6	1	4	61.02
7	2	0	91.75
8	2	2	89.66
9	2	4	88.99
19	0	0	1.61
20	0	2	2.72
21	0	4	3.69
22	1	0	59.11
23	1	2	60.31
24	1	4	61.10
25	2	0	91.23
26	2	2	89.82
27	2	4	88.60
37	0	0	1.63
38	0	2	3.06
39	0	4	3.87
40	1	0	58.99
41	1	2	60.62
42	1	4	61.27
43	2	0	90.90
44	2	2	89.58
45	2	4	88.72

The Fig. 9(a) shows the distribution of residuals versus fitted values, while Fig. 9(b) shows the same distribution on a log-normal distribution curve. As previously observed in Figs. 9(a) and 9(b), the residues are distributed following a normal distribution with low amplitude. To confirm this fact the histogram of the residues is showed in Fig 10.

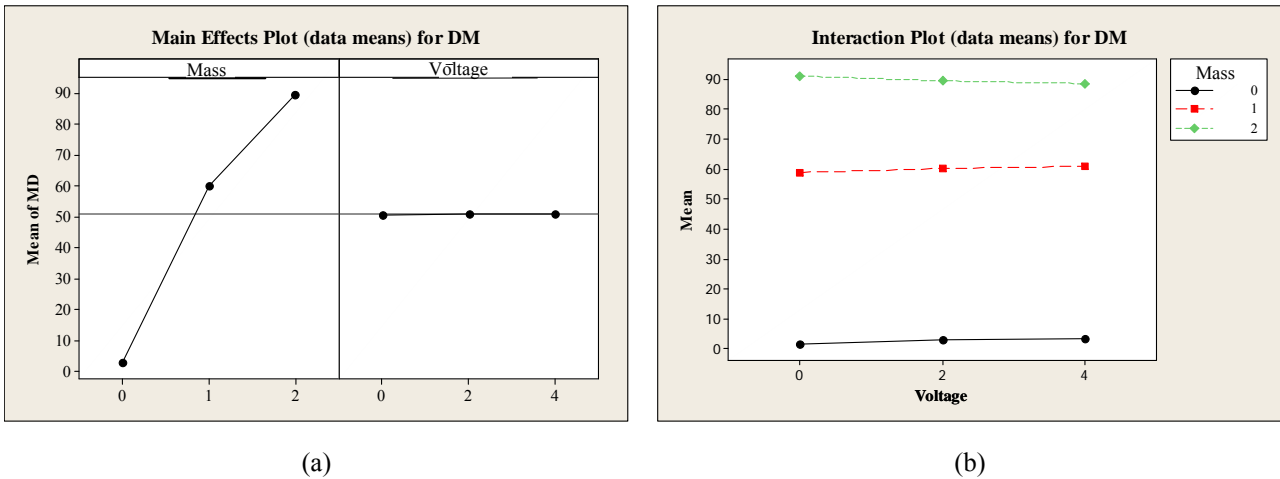


Figure 8 – Graphics of the main effect of the Meta-model; (a) Graphic of the isolated effects; (b) Graphic of cross effects.

The figure 11 show the data from the meta-model were obtained and analyzed by MINITAB. As described by the program, the meta-model has $R-Sq = 100,0\%$ and $R-Sq (adj) = 100\%$, representing a huge potential for representation of the meta-model of the second degree by experiments. The table 3 presents the results of the program of the adjusted values in a margin of 95% confidence.

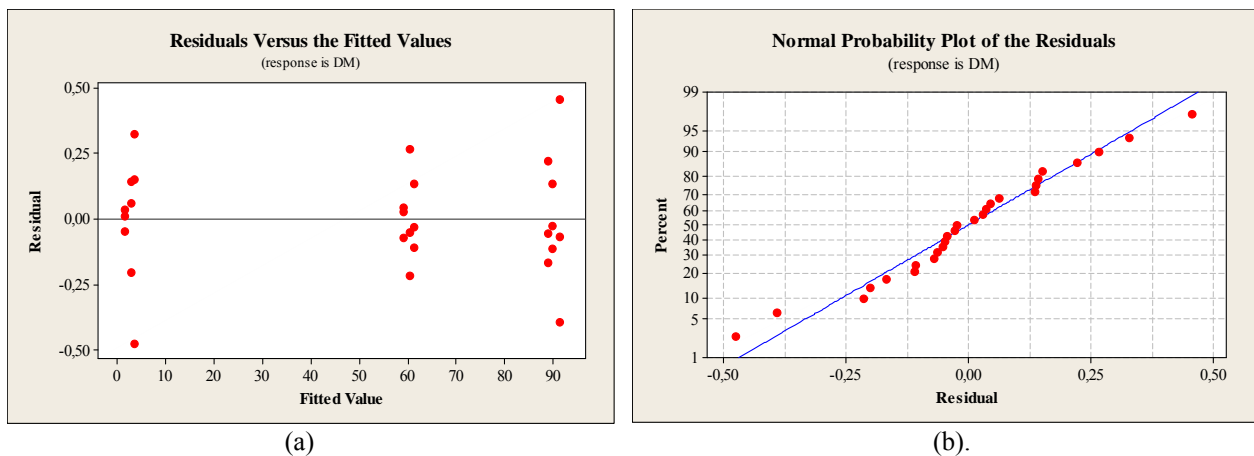


Figure 9. (a) Distribution of residuals versus fitted values; (b) Distribution of residuals by the normal probability curve.

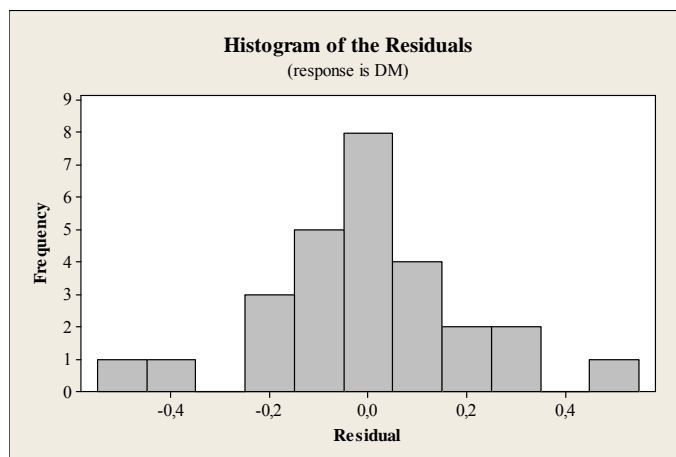


Figure 10. Histogram of Residuals.

Estimated Regression Coefficients for MD

Term	Coef	SE Coef	T	P
Constant	1.2896	0.30300	4.256	0.000
Mass	72.5019	0.52481	138.148	0.000
Voltage	0.7737	0.26241	2.949	0.008
Mass *Mass	-13.8849	0.23872	-58.165	0.000
Voltage*Voltage	-0.0228	0.05968	-0.383	0.706
Mass*Voltage	-0.5582	0.08440	-6.614	0.000

S = 0.5847 R-Sq = 100.0% R-Sq(adj) = 100.0%

Analysis of Variance for MD

Source	DF	Seq SS	Adj SS	Adj MS	F	P
Regression	5	35414.7	35414.75	7082.95	20715.87	0.000
Linear	2	34243.0	6569.81	3284.90	9607.53	0.000
Square	2	1156.8	1156.79	578.39	1691.66	0.000
Interaction	1	15.0	14.96	14.96	43.75	0.000
Residual Error	21	7.2	7.18	0.34		
Lack-of-Fit	3	6.1	6.12	2.04	34.64	0.000
Pure Error	18	1.1	1.06	0.06		
Total	26	35421.9				

Figure 11. Results from the analysis of meta-model data obtained and analyzed by MINITAB
 Table 3. Predicted response for new design points using model for MD

Point	Fit	SE Fit	95% CI	95% PI
1	1.2896	0.303000	(0.6595; 1.9197)	(-0.0800; 2.6592)
2	2.7457	0.251628	(2.2224; 3.2690)	(1.4219; 4.0695)
3	4.0191	0.303000	(3.3890; 4.6492)	(2.6495; 5.3887)
4	59.9066	0.251628	(59.3833; 60.4299)	(58.5828; 61.2304)
5	60.2462	0.251628	(59.7230; 60.7695)	(58.9224; 61.5701)
6	60.4031	0.251628	(59.8799; 60.9264)	(59.0793; 61.7270)
7	90.7539	0.303000	(90.1238; 91.3840)	(89.3843; 92.1235)
8	89.9771	0.251628	(89.4538; 90.5003)	(88.6532; 91.3009)
9	89.0175	0.303000	(88.3873; 89.6476)	(87.6479; 90.3870)
10	1.2896	0.303000	(0.6595; 1.9197)	(-0.0800; 2.6592)
11	2.7457	0.251628	(2.2224; 3.2690)	(1.4219; 4.0695)
12	4.0191	0.303000	(3.3890; 4.6492)	(2.6495; 5.3887)
13	59.9066	0.251628	(59.3833; 60.4299)	(58.5828; 61.2304)
14	60.2462	0.251628	(59.7230; 60.7695)	(58.9224; 61.5701)
15	60.4031	0.251628	(59.8799; 60.9264)	(59.0793; 61.7270)
16	90.7539	0.303000	(90.1238; 91.3840)	(89.3843; 92.1235)
17	89.9771	0.251628	(89.4538; 90.5003)	(88.6532; 91.3009)
18	89.0175	0.303000	(88.3873; 89.6476)	(87.6479; 90.3870)
19	1.2896	0.303000	(0.6595; 1.9197)	(-0.0800; 2.6592)
20	2.7457	0.251628	(2.2224; 3.2690)	(1.4219; 4.0695)
21	4.0191	0.303000	(3.3890; 4.6492)	(2.6495; 5.3887)
22	59.9066	0.251628	(59.3833; 60.4299)	(58.5828; 61.2304)
23	60.2462	0.251628	(59.7230; 60.7695)	(58.9224; 61.5701)
24	60.4031	0.251628	(59.8799; 60.9264)	(59.0793; 61.7270)
25	90.7539	0.303000	(90.1238; 91.3840)	(89.3843; 92.1235)
26	89.9771	0.251628	(89.4538; 90.5003)	(88.6532; 91.3009)
27	89.0175	0.303000	(88.3873; 89.6476)	(87.6479; 90.3870)

5. CONCLUSION

In this work the effects of electromagnetic fields was studied associated with electromechanical impedance signals in the process of monitoring of damages detection. It was considered the increase of the intensity of an electromagnetic field to the monitoring process (adding mass).

Looking at the regression model, there was a great influence of the mass factor for the monitoring process. It was observed in the experiment that the monitoring of structural changes did not suffer significant influence on the variation of electromagnetic field. This fact can be observed both by the coefficients of the meta-model based on regression, as the graphs of main effects.

However, this applications should be revised using others structure, using structural variation (mass) and environmental variation (intensity of electromagnetic field).

6. REFERENCES

- Liang. C., Sun. F.P., Rogers C.A. Coupled Electromechanical Analysis of Adaptive Material Systems – Determination of the Actuator Power Consumption and System Energy Transfer. *Journal of Intelligent Material Systems and Structures*. vol. 5. 12–20. 1994.
- Moura Jr. J.R.V. “Métodos de Identificação de Falhas em Estruturas Aeronáuticas Utilizando Meta-Modelagem Aliada às Técnicas de Impedância e Estruturas Inteligentes”. Dissertação de Mestrado. Faculdade de Engenharia Mecânica. Universidade Federal de Uberlândia. 2004.
- Moura Jr. J.R.V. ; Steffen Jr. V. . Impedance-Based Health Monitoring for Aeronautic Structures using Statistical Meta-modeling. *Journal of Intelligent Material Systems and Structures*. v. 17. p. 1023-1036. 2006.
- Park. G. Sohn. H., Farrar. C.R. and Inman. D.J.. “Overview of Piezoelectric Impedance-Based Health Monitoring and Path Forward”. *The Shock and Vibration Digest*. ol. 35. No. 6. November 2003. pp. 451-463. 2003.
- Rutherford. A.C., Park. G., Farrar. C.R.. “Non-linear Feature Identifications on Self-Sensing Impedance Measurements for Structural Health Monitoring”. *Mechanical System and Signal Processing*. Vol 21. pp. 322–333. 2007.
- Raju. V. Implementing impedance-based health monitoring. Master Thesis. Virginia Polytechnic Institute - State University. Blacksburg. USA. 1997.
- Sun. F.P., Chaudhry. Z., Liang. C., Rogers. C.A. Truss structure integrity identification using PZT sensor–actuator. *Journal of Intelligent Material Systems and Structures*. vol. 6. 134–139. 1995.

7. RESPONSIBILITY NOTICE

The authors are the only responsible for the printed material included in this paper.

8. ACKNOWLEDGMENTS

The first author is thankful to CAPES for her PhD scholarship. The authors acknowledge the support of FAPEMIG/CNPq.